

# NUMERICAL INVESTIGATION OF CAVITATION IN MULTI-DIMENSIONAL COMPRESSIBLE FLOWS

KRISTEN J. DEVAULT\*, PIERRE A. GREMAUD†, AND HELGE KRISTIAN JENSSEN‡

**Abstract.** The compressible Navier-Stokes equations for an ideal polytropic gas are considered in several space dimensions. The question of possible vacuum formation, an open theoretical problem, is investigated numerically using highly accurate computational methods (pseudospectral in space and high order in time). The flow is assumed to be symmetric about the origin with a purely radial velocity field. The numerical results indicate that there are weak solutions to the Navier-Stokes system in two and three space dimensions which display formation of vacuum when the initial data are discontinuous and sufficiently large. Various tests regarding mass conservation, energy balance, and comparison with the Euler equations suggest that the computed solutions correspond to solutions of the Navier-Stokes system. In addition, in the one-dimensional case, the numerical solutions are also in agreement with recent theoretical results.

**Key words.** Navier-Stokes, compressible flow, cavitation, pseudospectral

**AMS subject classifications.** 35Q30, 65M70, 76N99

**1. Introduction.** A long-standing open problem in the mathematical theory for fluid dynamics is the question of vacuum formation in compressible flow. Roughly stated the issue is: do there exist solutions of the Navier-Stokes system (3.1-3.3) for viscous compressible flow that exhibit vacuum (vanishing density) in finite time, when the initial density is strictly bounded away from zero?

This problem is relevant from a modeling perspective as well as for theoretical results. The underlying assumption in the derivation of the Navier-Stokes equations from physical principles is that the fluid is non-dilute and can be described as a continuum. A negative answer to the question above would thus provide self-consistency of the continuum assumption for the Navier-Stokes model. On the other hand, it is known that an *a priori* estimate of the form

$$\text{for a constant } C = C(T): \quad C^{-1} \leq \rho(x, t) \leq C \quad \text{for all } (x, t) \in \mathbb{R}^n \times [0, T], \quad (1.1)$$

( $\rho$  denotes density) implies further estimates, and would greatly facilitate existence proofs. For a discussion of this point see Chapter 3 of [10].

Estimates of the above type are available for one-dimensional (1D) flow [26], even in the case of large and rough data [15]. As reviewed in Section 2, large efforts have been invested in searching for similar bounds in the multi-dimensional (multi-D) case. However, no such results seem to be currently known.

To gain some insight, it is natural to first make a careful numerical study of the simplest possible scenario where one could expect cavitation in several space dimensions. This is the subject of the present work. In Section 3, we consider 2D and 3D flows with symmetry for the full Navier-Stokes equations, as well as for the barotropic

---

\*Department of Mathematics and Center for Research in Scientific Computation, North Carolina State University, Raleigh, NC 27695-8205, USA ([kjdevaul@ncsu.edu](mailto:kjdevaul@ncsu.edu)). Partially supported by the National Science Foundation (NSF) through grant DMS-0410561.

†Department of Mathematics and Center for Research in Scientific Computation, North Carolina State University, Raleigh, NC 27695-8205, USA ([gremaud@ncsu.edu](mailto:gremaud@ncsu.edu)). Partially supported by the National Science Foundation (NSF) through grants DMS-0244488 and DMS-0410561.

‡Department of Mathematics, Penn State University, University Park, State College, PA 16802, USA ([jenssen@math.psu.edu](mailto:jenssen@math.psu.edu)). Partially supported by the National Science Foundation (NSF) through grants DMS-0206631 and DMS-0539549 (CAREER).

case (where pressure is assumed to be a function of density alone). The equations are written in a proper non-dimensionalized form and the problem is completed with appropriate initial and boundary conditions. More is known in the formal limit of infinitely large Reynolds numbers, i.e., in the case of inviscid fluids. The corresponding Euler equations and their solutions are used as a benchmark for the numerics. Various considerations regarding the inviscid case are discussed in the Appendix.

The above difficulties are mirrored on the numerical side in the form of various challenges regarding stability. The case of 1D flows illustrates this issue. Riemann data with large jumps may lead to vacuum formation for the Euler equations while, at least for Hoff’s solutions [15], no vacuum is expected for solutions to the corresponding Navier-Stokes equations. Minimizing the amount of numerical diffusion is thus paramount. To do so, a highly accurate pseudospectral spatial discretization is used, see Section 4. The stiffness [1] of the discretized in time system increases as the density  $\rho$  goes to zero; for  $\rho = 0$ , the system is infinitely stiff and has degenerated from being purely differential to being differential algebraic. Several numerical schemes, none of them explicit, are known to handle this kind of difficulty [1, 12] (at least for some problems presenting this type of structure). A Backward Difference Formula (BDF) type method is considered here. This approach has been successfully tested with respect to mass conservation and energy balance. Finally, a test over the magnitude of the density has to be done to determine whether “vacuum” has been reached: an arduous task in finite precision computations! The numerical experiments are set up so that vacuum, if any, appears first at a known point (the origin). The calculations do not attempt to track the solution past vacuum formation. The detection of the vacuum itself, see criterion (5.1), is facilitated by the fact that for all the attempted experiments, there was a difference of at least 7 orders of magnitude on the size of the smallest observed density between the cases deemed to have vacuum formation versus those which did not.

Our detailed numerical study is described in Section 5. It indicates that vacuum formation indeed occurs for multi-D symmetric flows for sufficiently large and discontinuous initial data, i.e., in the regime of high Mach number and high Reynolds number. Section 6 contains a brief summary and a conclusion of our findings.

## 2. Challenges and relation to other works.

**2.1. Theoretical issues.** There is a voluminous literature on compressible flow. A short review of work relevant to vacuum formation and *a priori* estimates follows.

**2.1.1. 1D flows.** For one-dimensional flow, i.e. multi-D flow with planar symmetry, much stronger results are known than what is currently available for higher dimensions. A seminal work of Kazhikhov & Shelukhin [26] considers the full 1D Navier-Stokes system for an ideal polytropic gas. Building on earlier work by Kanel [21] and Kazhikhov [25], the global existence and uniqueness of a smooth ( $W^{1,2}$ ) solution is proved in [26] for arbitrarily large and smooth data. In particular, *a priori* bounds of the type (1.1) are established. Similar results for more general gases can be found in [3], [4], [24].

Highly relevant to the present work is an extension to large and rough (possibly discontinuous) data established by Hoff [15]. This result pertains to isentropic or isothermal flow with data  $(\rho_0, u_0)$  satisfying

$$\rho_0 \in L^\infty(\mathbb{R}), \quad \text{ess inf}_{\mathbb{R}} \rho_0 > 0,$$

and

$$\rho_0 - \bar{\rho}, \quad u_0 - \bar{u} \in L^2(\mathbb{R}),$$

where  $\bar{\rho}, \bar{u}$  are monotone functions that agree outside a bounded interval with the limiting values of  $\rho$  and  $u$  at  $\pm\infty$ . Hoff [15] proves that there exists a global weak solution which satisfies (1.1). This result shows that there is at least one solution of the Navier-Stokes equations that does not exhibit cavitation, even for Riemann type data with arbitrarily large jumps. (For an extension of this result to certain flows for the full Navier-Stokes system see [20]). This is in contrast to the 1D inviscid Euler equations, for which it is well-known that vacuum formation can occur [34]. The present numerical study does not contradict Hoff's result. Indeed, while our results clearly indicate the possibility of vacuum formation in higher dimensions, we have not numerically observed cavitation in solutions of the 1D Navier-Stokes system.

A significant result concerning cavitation in 1D flow is given by Hoff & Smoller [19]. They demonstrate that any, everywhere defined, weak solution of the Navier-Stokes (barotropic or full) system which satisfies some natural, weak integrability assumptions cannot contain a vacuum in a non-empty open set, unless the initial data do so. (For a recent refinement of this result see [8].)

**2.1.2. Multi-D flows.** Much less is known about compressible flow in higher dimensions. Global existence of weak solutions is a formidable problem and the theory is far from complete. Roughly speaking currently known results are of two types: (A) for large and rough data that possibly contain vacuum states, and (B) for small, rough data with  $\text{ess inf } \rho_0 > 0$ . (We do not review results on local existence; see the recent monograph [31] for an extensive bibliography.)

In the former case, P.L. Lions [27] has established existence of global weak solutions in the case of compressible, barotropic flow. For recent extensions, including results for the full Navier-Stokes system, see [9], [10] and references therein. It is not known if a bound of the type (1.1) holds for these solutions when the data satisfy  $\text{ess inf } \rho_0 > 0$ .

More is known for "small" data, i.e. data close to a constant state in a suitable norm. In particular, small and sufficiently smooth data generate global smooth solutions without cavitation for the full Navier-Stokes system [30], [22], [23]. For a representative result in the case of barotropic flow see Chapter 9 in [31]. In a series of papers Danchin, [5], [6], [7], has established global existence, and also uniqueness, of compressible flows in several space dimensions for solutions in so-called critical spaces. For flows with even less regularity, possibly with discontinuities across hypersurfaces, Hoff [14] has shown that if the data are sufficiently close to a constant state, in a suitable norm, and with initial density and temperature bounded away from zero, then there exists a global weak solution with the same properties at all later times. No corresponding result seems to be known for large data in several space dimensions.

There are somewhat stronger results available for the type of symmetric (quasi 1D) flows we consider in this paper. For isothermal flow with spherical symmetry, Hoff [13] establishes existence of a global weak solution for large, symmetric data. The solution is obtained as the limit of solutions in shells  $\{0 < a \leq r \leq b\}$  as  $a \downarrow 0$ . By rewriting the equations in Lagrangian coordinates and exploiting the energy estimate, certain *a priori* bounds are obtained that are independent of the inner radius  $a$ . However, while guaranteeing existence of a weak solution, the available *a priori* bounds do not seem strong enough to determine whether the constructed solution

contains a vacuum at the center of motion. (For an extension of this result to the full Navier-Stokes system see [17].)

We note that the higher the dimension of the ambient space, the easier it should be to generate a vacuum. Roughly speaking, in higher dimensions there are more directions for the fluid to move in and it should be relatively easier to attain low densities. This can be verified for the corresponding inviscid system. Indeed, consider the isentropic Euler equations with spherically symmetric Riemann-type data. Let the initial velocity field have constant magnitude  $\bar{u}$  and be directed radially away from the origin. In this case, there is a threshold value  $\hat{u}(n)$  of  $\bar{u}$ , depending on the dimension  $n$  of the ambient space, above which a vacuum is formed immediately [40]. One can verify that  $\hat{u}(1) > \hat{u}(2) > \hat{u}(3)$ . For the 1D Navier-Stokes system, we know from Hoff's result [13] that there exists a weak solution without vacuum, i.e. " $\hat{u}(1) = \infty$ " for these solutions. However, in higher dimensions it may well be that there are solutions with strictly positive density everywhere at time zero, but which develop a vacuum at later times<sup>1</sup>. There are also technical reasons that seem to prevent *a priori* bounds on the density in higher dimensions. More precisely, in the 1D analysis of [26], [13] the bounds on the density are derived from the *a priori* bounds one gets "for free" from the equations themselves. These are integral bounds that are strictly stronger in 1D than in higher dimensions due to the geometrical factor of  $r^{n-1}$  in the space integrals (i.e.  $dx = \text{const.} r^{n-1} dr$ ).

## 2.2. Additional remarks.

*Cavitation and uniqueness.* The issue of cavitation is closely related to the question of uniqueness and to the concept of solution one works with. To illustrate this consider the 1D Navier-Stokes equations with Riemann type data

$$\rho_0(x) \equiv \bar{\rho} > 0, \quad u_0(x) = \begin{cases} -\bar{u} & \text{for } x < 0, \\ \bar{u} & \text{for } x > 0, \end{cases} \quad (2.1)$$

where  $\bar{u} > 0$ . One weak solution to this problem is provided by Hoff's result [15], and this solution does not exhibit cavitation. However, a different solution can also be constructed, with the same data, by piecing together solutions of two disjoint flows into surrounding vacuum. More precisely, consider the two sets of initial data

$$\rho_0^-(x) = \begin{cases} \bar{\rho} & \text{for } x < 0, \\ 0 & \text{for } x > 0, \end{cases} \quad u_0^-(x) = \begin{cases} -\bar{u} & \text{for } x < 0, \\ \emptyset & \text{for } x > 0, \end{cases} \quad (2.2)$$

and

$$\rho_0^+(x) = \begin{cases} 0 & \text{for } x < 0, \\ \bar{\rho} & \text{for } x > 0, \end{cases} \quad u_0^+(x) = \begin{cases} \emptyset & \text{for } x < 0, \\ \bar{u} & \text{for } x > 0. \end{cases} \quad (2.3)$$

(Here  $\emptyset$  indicates that the velocity is left undefined where there is no matter.) One can now construct solutions  $(\rho^-, u^-)$  and  $(\rho^+, u^+)$  corresponding to these data, that in addition satisfy a physical no-traction boundary condition along a vacuum-fluid interface, see [3], [4], [24], [25]. By concatenating the two solutions a solution to the original problem (2.1) is obtained, and in this solution an open vacuum region is present from time  $t = 0+$  (and staying at least for a short time). In the region between the two solutions, one may simply consider the flow to be undefined. Without going

<sup>1</sup>Furthermore, the possibility remains that there are other weak solutions exhibiting vacuum even in 1D (see below for further comments on uniqueness).

into the discussion of which solution is more relevant, we note that Hoff’s solution [15] is defined *everywhere* on  $\mathbb{R} \times \mathbb{R}_+$ , while the second solution is defined only on the support of its density. The issue of non-uniqueness for 1D compressible Navier-Stokes in connection with vacuums is treated in detail by Hoff & Serre [18].

For flow in several space dimensions, the picture is less clear since we do not even know if there is a solution without cavitation in this case. The present work indicates that there is at least one solution where a vacuum forms. Uniqueness of *general* weak solutions, i.e. without any further regularity assumptions beyond what is necessary to make sense of a weak formulation, is not known. On the other hand, sufficiently smooth and small solutions are unique, see [30], as are flows belonging to critical spaces, Danchin [5], [6], [7]. To the best of our knowledge, the only uniqueness result for flows with possible discontinuities in the density field is given in a recent work by Hoff [16]. There, uniqueness is established under certain assumptions, among them that a bound of the type (1.1) holds for at least one of the solutions under consideration.

*Continuum assumption and physical boundary conditions.* In view of the 1D examples above, one should be cautious in making claims about the “physicality” of constructed or computed solutions to the standard Navier-Stokes model (3.1-3.3) in the low-density regime. Of course, from a modeling point of view, this is not surprising. The Navier-Stokes system is derived under the assumption that the fluid can be described as a continuum with everywhere strictly positive mass density. Issues related to non-uniqueness in presence of vacuum is therefore not surprising. For a discussion of this point, see [10]. It is also known [35] that the lifespan of smooth, everywhere defined solutions to the Navier-Stokes system (with vanishing heat conductivity) is finite whenever the initial density is compactly supported.

Once a vacuum has developed, one should impose the physical boundary condition of vanishing traction at the vacuum-fluid interface. In other words, the vacuum should not exert a force on the fluid. Note that in the present work, we track the *onset* of vacuum formation, not its subsequent evolution.

*Well-posedness.* In view of both physical arguments as well as the apparent lack of good *a priori* estimates for the standard Navier-Stokes model, it is natural to ask if more accurate models would lead to stronger results. In particular, models where the transport coefficients  $\lambda$ ,  $\mu$ ,  $\kappa$  depend on the thermo-dynamical state could be considered<sup>2</sup>. Several issues pertaining to the well-posedness in the presence of vacuum have been analyzed in [28], [29], [36], [37], [38], [39]. These results show that the non-uniqueness observed in [18] can be attributed to the unphysical assumption of constant viscosity coefficient. The corresponding problem for the full system appears to require new methods. Concerning results in this direction for the full 1D system see [3], [4], [24], and the recent monograph by Feireisl [10] for the multi-D case.

*Precise formulation.* After the above remarks, our original question can be formulated more precisely as follows. Given the standard, multi-dimensional Navier-Stokes model with constant transport coefficients, let the pressure be that of an ideal polytropic gas or, in the case of barotropic flow, of the form  $A\rho^\gamma$  with  $\gamma \geq 1$ . Consider the initial-boundary value problem in a ball centered at the origin, with initial density strictly bounded away from zero and with a possibly discontinuous initial velocity field. Then: *Does there exist an everywhere defined weak solution of the equations with the property that its density reaches zero in finite time?*

---

<sup>2</sup>In the 1D isentropic case a relevant assumption is that the viscosity  $\mu$  depends on the density. In accordance with kinetic theory it is natural to consider the case with  $\mu \sim \rho^k$ , for a constant  $k > 0$ .

**3. The full compressible Navier-Stokes equations.** Consider the compressible Navier-Stokes equations for a Newtonian fluid in  $\mathbb{R}^n$ ,  $n = 1$ ,  $n = 2$  or  $n = 3$  with no external forces or heat sources. The invariant form of the equations in spatial (Eulerian) formulation is

$$\rho_t + \operatorname{div}(\rho \vec{u}) = 0 \quad (3.1)$$

$$(\rho \vec{u})_t + \operatorname{div}(\rho \vec{u} \otimes \vec{u}) = \operatorname{grad}(-p + \lambda \operatorname{div} \vec{u}) + \operatorname{div}(2\mu D) \quad (3.2)$$

$$\mathcal{E}_t + \operatorname{div}((\mathcal{E} + p)\vec{u}) = \operatorname{div}(\lambda(\operatorname{div} \vec{u})\vec{u} + 2\mu D \cdot \vec{u} - \vec{q}) \quad (3.3)$$

where  $\rho$  is the density,  $\vec{u} = (u_1, \dots, u_n)^T$  is the fluid velocity,  $p$  is the pressure,  $\mathcal{E}$  is the total energy,  $D$  is the deformation rate tensor,  $\vec{q}$  is the heat flux vector, and  $\lambda$  and  $\mu$  are the viscosity coefficients. Equations (3.1-3.3) are often referred to as the continuity equation, the conservation of momentum equation, and the conservation of energy equation, respectively. We also have

$$\mathcal{E} = \rho(e + |\vec{u}|^2/2), \quad D = (\partial_i u_j + \partial_j u_i)/2, \quad \vec{q} = -\kappa \nabla \theta,$$

where  $e$  stands for the internal energy,  $\kappa$  is the coefficient of heat conductivity, and  $\theta$  is the temperature. In what follows, we restrict ourselves to the study of ideal and polytropic (perfect) gases such that

$$p = \mathcal{R}\rho\theta, \quad e = c_v\theta, \quad (3.4)$$

where  $\mathcal{R}$  is the gas constant and  $c_v$  is the specific heat at constant volume. The local sound speed  $c$  is then given by

$$c = \sqrt{\frac{\gamma p}{\rho}},$$

where  $\gamma = 1 + \mathcal{R}/c_v$  is the adiabatic exponent. All the transport coefficients  $c_v$ ,  $\lambda$ ,  $\mu$ ,  $\kappa$  are assumed to be constant. For the derivation of the equations see e.g. [31, 32].

**3.1. Equations for symmetric flow.** We next consider the case of flow with symmetry, i.e. the velocity is directed (radially when  $n = 2, 3$ ) away from the origin and all quantities are functions only of the distance to the origin, and time. Let  $x$  denote a point in space and set  $r = |x|$ . Setting

$$\rho(r, t) = \rho(x, t), \quad \vec{u}(x, t) = u(r, t)\frac{x}{r}, \quad \text{etc.}\dots$$

leads to the following system of equations,

$$\rho_t + (\rho u)_\xi = 0 \quad (3.5)$$

$$\rho(u_t + uu_r) + p_r = \nu u_{\xi r} \quad (3.6)$$

$$c_v \rho(\theta_t + u\theta_r) + pu_\xi = \kappa \theta_{r\xi} + \nu(u_\xi)^2 - \frac{2m\mu}{r^m}(r^{m-1}u^2)_r, \quad (3.7)$$

where we have used the notation

$$m = n - 1, \quad \partial_\xi = \partial_r + \frac{m}{r}, \quad \nu = \mu + 2\lambda.$$

(Note that  $\partial_{\xi r} \neq \partial_r \xi$  for  $n = 2$  and  $n = 3$ .)

We consider spherically symmetric flows (3.5)-(3.7) in the interior of the interval/disk/ball  $B_b$  of fixed outer radius  $b$

$$\rho(r, 0) = \rho_0(r), \quad u(r, 0) = u_0(r), \quad \theta(r, 0) = \theta_0(r), \quad \text{for } r \leq b. \quad (3.8)$$

In the one-dimensional case we require that (3.8) holds for all  $|r| \leq b$ . Throughout, we only consider the case where the gas is set in motion in the outward direction, i.e. we assume that  $u_0$  is a non-negative function in 2D and 3D and is odd with positive values for  $r > 0$  in 1D. Suitable boundary conditions are discussed in 3.4.

**3.2. Non-dimensional form of symmetric equations.** Using the initial data, characteristic length, velocity, density, and temperature can be defined

$$\begin{aligned} \bar{r} &:= b, \\ \bar{u} &:= \max_{0 \leq r \leq b} |u_0(r)|, \\ \bar{\rho} &:= \max_{0 \leq r \leq b} \rho_0(r), \\ \bar{\theta} &:= \max_{0 \leq r \leq b} \theta_0(r). \end{aligned}$$

From these we define characteristic time and pressure by

$$\begin{aligned} \bar{t} &:= \frac{\bar{r}}{\bar{u}}, \\ \bar{p} &:= p(\bar{\rho}, \bar{\theta}). \end{aligned}$$

The dimensionless independent variables are then

$$R := \frac{r}{\bar{r}}, \quad T := \frac{t}{\bar{t}},$$

and the dimensionless dependent variables are

$$D := \frac{\rho}{\bar{\rho}}, \quad U := \frac{u}{\bar{u}}, \quad \Theta := \frac{\theta}{\bar{\theta}}, \quad P := \frac{p}{\bar{p}}.$$

Regarding  $D$ ,  $U$ ,  $\Theta$ ,  $P$  as functions of  $R$  and  $T$ , we obtain the non-dimensionalized system

$$\rho_t + (\rho u)_\xi = 0 \quad (3.9)$$

$$\rho(u_t + uu_r) + \frac{1}{\gamma M^2} (\rho \theta)_r = \frac{1}{\text{Re}} u_{\xi r} \quad (3.10)$$

$$\begin{aligned} \rho(\theta_t + u\theta_r) + (\gamma - 1)\rho\theta u_\xi &= \frac{1}{\text{Pr Re}} \theta_{r\xi} \\ &+ \gamma(\gamma - 1) \frac{M^2}{\text{Re}} \left( (u_\xi)^2 - \frac{2m\mu}{\nu} \frac{(r^{m-1}u^2)_r}{r^m} \right), \end{aligned} \quad (3.11)$$

where we have reverted to the original symbols and where

$$\begin{aligned} M &:= \frac{|\bar{u}|}{\bar{c}} = \text{Mach number} & \bar{c} &= \text{sound speed} = \sqrt{\frac{\gamma \bar{p}}{\bar{\rho}}}, \\ \text{Re} &:= \frac{\bar{r} \bar{\rho} \bar{u}}{\nu} = \text{Reynolds number}, \\ \text{Pr} &:= \frac{\nu c_v}{\kappa} = \text{Prandtl number}. \end{aligned}$$

These equations are valid also for  $n = 1$  ( $m = 0$ ) provided  $r$  is interpreted as the position along the  $x$ -axis; in this case  $\partial_\xi = \partial_r = \partial_x$ .

**3.3. Barotropic equations.** If the pressure  $p$  is considered as a function of the density  $\rho$  only, the energy equation (3.7) decouples from the mass and momentum conservation equations (3.5, 3.6). Here, we consider exclusively the isentropic and isothermal cases where

$$p(\rho) = a\rho^\gamma \quad \gamma \geq 1, \quad (3.12)$$

and where  $a > 0$  is a constant. A nondimensional version of the barotropic equations can be derived in very much the same way as (3.9-3.11) were derived, except for the characteristic pressure which is now taken as

$$\bar{p} = p(\bar{\rho}) = a\bar{\rho}^\gamma.$$

This leads to the non-dimensionalized system for barotropic flow

$$\rho_t + (\rho u)_\xi = 0, \quad (3.13)$$

$$\rho(u_t + uu_r) + \frac{1}{\gamma M^2}(\rho^\gamma)_r = \frac{1}{\text{Re}}u_{\xi r}, \quad (3.14)$$

where the Mach number at the reference state is now given by

$$M := \frac{|\bar{u}|}{\bar{c}} = \frac{|\bar{u}|}{a\gamma\bar{\rho}^{\gamma-1}}.$$

**3.4. Boundary conditions and balance relations.** The following initial and boundary conditions are considered throughout

$$\rho(r, 0) = \rho_0(r) = 1 \text{ for } r \geq 0, \quad u(r, 0) = u_0(r) = \begin{cases} 1 & \text{if } r > 0, \\ 0 & \text{if } r = 0, \end{cases} \quad (3.15)$$

$$u(1, t) = 1, \quad t > 0, \quad (3.16)$$

where  $r = 1$  corresponds now to the outer boundary of the computational domain. Furthermore, by symmetry, one has

$$u(0, t) = 0, \quad t > 0, \quad (3.17)$$

It may have been more natural to consider a homogeneous condition of the type  $u(1, t) = 0$  instead of (3.16) since that is the case where existence of weak solutions has been established. There are two reasons not to do this. First, such a condition would lead to steep gradients and unwanted boundary layer effects on the outer boundary of the domain. It would thus complicate the numerical resolution of the problem by making it more susceptible to spurious oscillations. Second, under the above type of initial conditions (3.15), vacuum formation, if any, is expected to be initiated at the origin (see Section 5). For short time intervals one would therefore expect that the outer boundary condition does not play a significant role in the behavior of the solution near the origin.

Global balance relations for mass and energy can be inferred from the above system. If  $\mathcal{M}(t)$  denotes the total mass in the domain  $\{0 < r < 1\}$  then by (3.13) and (3.16), we have

$$\mathcal{M}(t) = \mathcal{M}(0) - c_m \int_0^t \rho(1, \tau) d\tau \quad \text{with } c_m = \begin{cases} 1 & \text{if } m = 0, \\ 2\pi & \text{if } m = 1, \\ 4\pi & \text{if } m = 2. \end{cases} \quad (3.18)$$

An energy balance is obtained by multiplying equation (3.13) by  $\frac{u^2}{2}$  and equation (3.14) by  $u$ , adding, and integrating with respect to space and time. Taking into account the side conditions (3.15-3.17) leads to the following energy balance

$$\int_0^1 \left( \frac{1}{2} \rho u^2 + G(\rho) \right) r^m dr + \frac{1}{\text{Re}} \int_0^t \int_0^1 \left( u_r^2 + \frac{m}{r^2} u^2 \right) r^m dr d\tau = \frac{1}{2n} - \int_0^t \left[ \frac{1}{2} \rho(1, \tau) + G(\rho(1, \tau)) + \frac{1}{\gamma M^2} \left( \rho(1, \tau)^\gamma - 1 \right) - \frac{1}{\text{Re}} u_r(1, \tau) \right] d\tau, \quad (3.19)$$

where

$$G(\rho) = \frac{\rho}{\gamma M^2} \int_1^\rho \frac{s^\gamma - 1}{s^2} ds$$

is the potential energy.

**4. Discretization and numerical analysis.** The equations are discretized in space using Chebyshev collocation methods [2]. Such methods deliver high accuracy with a low number of nodes for smooth solutions (which are expected here). Unlike the two and three dimensional cases, the one-dimensional case does not have a coordinate singularity at  $r = 0$ . The discretization reflects this. In the one-dimensional case, Chebyshev collocation is done at the usual Chebyshev-Gauss-Lobatto nodes in the spatial domain  $(0, 1)$

$$r_j = \frac{1}{2} \left( 1 + \cos \left( \frac{\pi j}{N-1} \right) \right), \quad j = 0, \dots, N-1,$$

while in the two and three dimensional cases, the Chebyshev-Gauss-Radau nodes are used instead

$$r_j = \frac{1}{2} \left( 1 + \cos \left( \frac{2\pi j}{2N-1} \right) \right), \quad j = 0, \dots, N-1.$$

In each case,  $N$  stands for the number of nodes. If  $v$  is any of the above unknowns to be determined for  $r \in (0, 1)$  and  $t > 0$ , we seek an approximation of it of the form

$$v_N(r, t) = \sum_{i=0}^{N-1} V_i(t) \psi_i(r),$$

where  $\{\psi_i\}_{i=0}^{N-1}$  are the Lagrange interpolation polynomials at the Chebyshev-Gauss-Lobatto/Radau nodes on  $[0, 1]$ , i.e.,  $\psi_i(x_j) = \delta_{ij}$ .

Interpolation at one of the above sets of nodes of a function  $v = v(r, t)$  simply takes the form

$$I_N v(r, t) = \sum_{j=0}^{N-1} v(r_j, t) \psi_j(r).$$

By definition, the Chebyshev collocation derivative of  $v$  with respect to  $r$  at those nodes is then

$$\frac{\partial}{\partial r} (I_N v)(r_l, t) = \sum_{j=0}^{N-1} v(r_j, t) \psi_j'(r_l) = \sum_{j=0}^{N-1} D_{lj} v(r_j, t),$$

with  $D_{lj} = \psi'_j(r_l)$ . The collocation derivative at the nodes can then be obtained through matrix multiplication.

For the sake of simplicity, we only describe the discretization process for the barotropic equations. The discretization of the full system relies on identical principles and can easily be derived by the reader. Approximations for the density  $\rho$  and the velocity  $u$  are taken as

$$\rho_N(r, t) = \sum_{i=0}^{N-1} V_i(t)\psi_i(r), \quad \text{and} \quad u_N(r, t) = \sum_{i=0}^{N-1} U_i(t)\psi_i(r).$$

The semi-discretized in space problem (3.13, 3.14) has the form

$$Z_V (V' + DU.*V + U.*DV + mU.*V./R) = B_V, \quad (4.1)$$

$$Z_U \left( V.*(U' + U.*DU) + \frac{1}{\gamma M^2} D(V.\hat{\gamma}) - \frac{1}{Re} [D^2U + m(DU)./R - mU./(R.\hat{2})] \right) = B_U, \quad (4.2)$$

with the obvious notation for  $U$ ,  $V$  and  $D$ ; the vector  $R$  is the node vector,  $R_j = r_j$ ,  $j = 0, \dots, N-1$ . The matrices  $Z_V$  and  $Z_U$  zero the first and/or the last entry(ies) of a vector, further  $B_V$  and  $B_U$  are two vectors related to the boundary conditions (to be specified below). In the above equations, a “dotted operation” (for instance  $.*$ ) refers to that operation being performed elementwise (for instance,  $U.*V$  is the vector of  $i$ -th component  $U_i V_i$ ,  $i = 0, \dots, N-1$ ).

The computations are carried out with the boundary condition (3.16). Such a boundary condition corresponds to one algebraic equation; the corresponding nodal unknown may be eliminated. Equations (4.1, 4.2) result then in a system of the type

$$\begin{bmatrix} \mathbb{I} & 0 \\ 0 & \text{diag}(\mathcal{V}) \end{bmatrix} \begin{bmatrix} \mathcal{V}' \\ \mathcal{U}' \end{bmatrix} = \mathcal{F}(\mathcal{U}, \mathcal{V}), \quad (4.3)$$

where  $\mathcal{U}$  and  $\mathcal{V}$  are the remaining unknowns after the boundary conditions have been taken into account and where  $\mathcal{F}$  is a known nonlinear function easily derived from (4.1) and (4.2) and the boundary conditions. In (4.3),  $\text{diag}(\mathcal{V})$  stands for the diagonal matrix having  $\mathcal{V}$  as its diagonal.

In case the density vanishes (or becomes very small) at some node  $r_i$  at time  $t$ , i.e.,  $\mathcal{V}_i(t) = 0$ , then the differential equation for  $\mathcal{U}_i(t)$  degenerates into an algebraic equation; in other words, the system (4.3) becomes differential algebraic. How much of a numerical problem this is depends on the index of the system. The minimum number of times one has to differentiate all or part of (4.3) to recover an ODE system is the index of the Differential Algebraic Equation (DAE) [1]. Here the index is easily found to be equal to one. Indeed, differentiating the algebraic equation for  $\mathcal{U}_i$  leads to an ODE provided the operator  $D^2 + m \text{diag}(1./R)D - m \text{diag} 1./(R.\hat{2})$  with proper side conditions applied to  $U'$  is nonsingular. The side conditions are that the velocity is fixed on the outer boundary and thus  $U'_1(t) = 0$  and that nonsingular solutions are sought. The above operator can be checked to be nonsingular by direct inspection of the matrices involved. Alternatively, at the continuous level, one can check that the only nonsingular solution to  $\partial_{rr}\dot{u} + m/r\partial_r\dot{u} - m\dot{u}/r^2 = 0$  with  $\dot{u}(1) = 0$  is the trivial solution  $\dot{u} \equiv 0$  (where  $\dot{u} = u_t$ ).

In the presence of vacuum, the system (4.3) is a semi-explicit of index 1 DAE, as such it is amenable to relatively simple time discretization such as BDF [1]. Here, the MATLAB routine ODE15s which implements a variant of BDF was used [33].

Several aspects of the numerical approach can be tested for validity and efficiency. For instance, the global balance relations (3.18, 3.19) derived for the mass and energy can be tested on the numerical solutions. The residuals corresponding to the evaluation of each relation, i.e., when  $u$  and  $\rho$  are replaced by  $u_N$  and  $\rho_N$ , have been checked to be of order  $10^{-6}$  and  $10^{-8}$  in the maximum norm (in time) for the mass and energy balance, respectively.

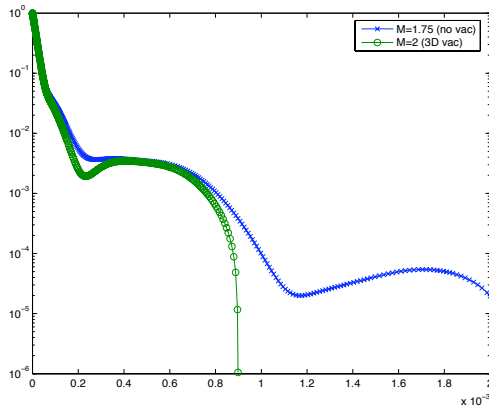


FIG. 5.1. Time behavior of the density at the node closest to the origin, i.e.,  $\rho_N(r_{N-1}, \cdot)$  for the three-dimensional barotropic equations with  $Re = 45000$ ,  $\gamma = 1.4$  and  $M = 1.75$  and  $M = 2$ .

**5. Numerical results.** The problem (3.13, 3.14) has been solved using the method described in the previous section with various values of the physical parameters (Mach number  $M$ , Reynolds number  $Re$ , and adiabatic coefficient  $\gamma$ ). The initial and boundary conditions are given by (3.15) and (3.16) respectively. The mesh size is fixed at  $N = 128$  for all the results given below.

For all our examples, the numerical density  $\rho_N$  is an increasing function of  $r$  and thus the numerical solution is probed at the node closest to the origin for vacuum detection. Vacuum formation, if it occurs, is expected to take place during a fast initial transient phase. A comparison with the inviscid case is instructive. If cavitation takes place for the Euler equations, it does so instantaneously (at the origin), i.e., for  $t > 0$ . For the one-dimensional case, this fact is obvious from the explicit self-similar solutions given in the Appendix; for the multidimensional case, see [40], Section 7.10.1. Regarding the Navier-Stokes equations, our efforts are concentrated on the multidimensional cases for which there is no node at the origin. It is observed numerically that near the origin the density either abruptly dives down to “zero” or slowly decreases. This behavior is illustrated by Figure 5.1. The non-monotonous character of the evolution in the figure is due to the nature of the spatial discretization, more precisely the interaction of the outgoing waves with the successive nodes.

Based on the above remarks, a specific calculation is said to lead to vacuum formation if for some time  $t$ ,  $0 < t < .002$

$$\rho_N(r_{N-1}, t) < tol = 10^{-10}, \quad (5.1)$$

where  $r_{N-1} = \frac{1}{2}(1 + \cos(\frac{2N-1}{2N-2}\pi))$  is the Chebyshev-Gauss-Radau node closest to the origin.

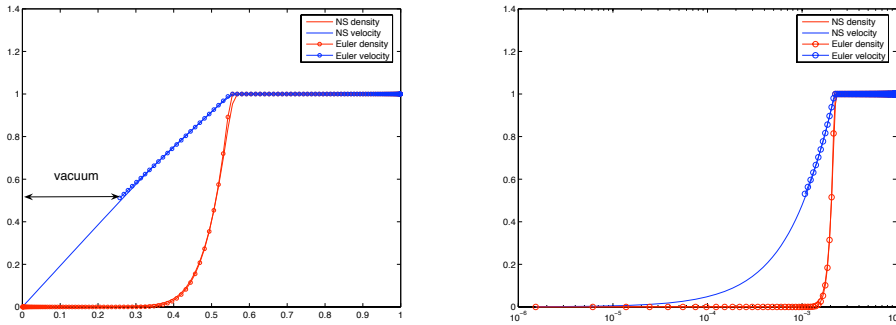


FIG. 5.2. *One-dimensional Navier-Stokes and Euler solutions for  $\gamma = 1.4$ ,  $M = 10$ . Left: solutions at time  $t = 0.5$  with  $Re = 10,000$  (for the Navier-Stokes flow); right: solutions at time  $t = .002$  with  $Re = 1,000,000$  (for the Navier-Stokes flow). For these values, both the one-dimensional Euler solution and the multidimensional Navier-Stokes exhibit cavitation (see Figure 5.4 below), while the 1D Navier-Stokes solution does not.*

**5.1. The one-dimensional case.** The one-dimensional calculations were found to be more sensitive to numerical instabilities than their higher dimensional counterparts. To counterbalance this, the one-dimensional computational domain was in some cases truncated to concentrate on the neighborhood around the origin. In essence, this refines the mesh near  $r = 0$  and gets rid of the part of the domain where the solutions are roughly constant. All the multidimensional calculations are obtained on the full spatial domain  $0 < r < 1$ . In Figure 5.2, two one-dimensional cases are illustrated for the values  $\gamma = 1.4$  and  $M = 10$ . The left picture shows the behavior of the solution at  $t = .5$  for a “mild” Reynolds number of  $Re = 10,000$ . The local behavior near the origin is illustrated in Figure 5.2, right, for  $Re = 1,000,000$  and at time  $t = .002$ . For illustration purposes, the corresponding Euler solutions are also displayed. The Euler solutions are exact, see Appendix. The parameters are such that cavitation occurs for the Euler flow ( $M > \frac{2}{\gamma-1}$ ). No vacuum formation was observed for the one-dimensional Navier-Stokes solution; in fact, the minimum value of the density is of order .001, seven order of magnitude larger than the threshold used above in (5.1). The absence of vacuum in the solutions to the 1D Navier-Stokes system is consistent with the solutions found by Hoff [15] who considers discontinuous data of the same type as in the present paper.

**5.2. The multidimensional barotropic case.** The two- and three-dimensional barotropic flows (3.13, 3.14) with initial and boundary conditions (3.15, 3.16) are solved, for fixed values of the adiabatic coefficient  $\gamma$  on grids in “Reynolds and Mach number space”, i.e., for a collection of values of those two parameters.

Figure 5.3 corresponds to the value  $\gamma = 1$  for the two- and three-dimensional cases. The minimum of the density at the node closest to the origin, see criterion (5.1), is displayed in Figure 5.3, left (for the 3D case). Figure 5.3, right, gives a more detailed description of the values of  $M$  and  $Re$  leading to cavitation: values “above” the two curves lead to vacuum. It clearly illustrates that for large enough values of both  $M$  and  $Re$ , there appears to be vacuum formation. The displayed results are not

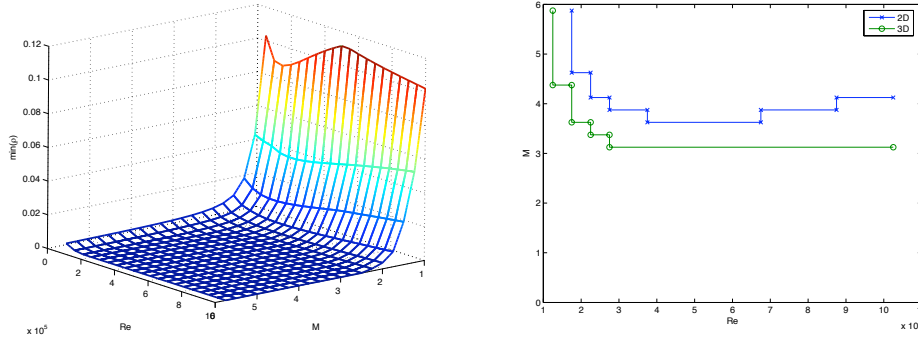


FIG. 5.3. Vacuum formation for two- and three-dimensional barotropic flows (3.13, 3.14) with initial and boundary conditions (3.15, 3.16) and  $\gamma = 1$ . Left: minimum value of the density for the 3D problem; right: vacuum formation for 2D and 3D. Vacuum occurs for values of the parameters corresponding to points above the curves.

strongly sensitive to the choice of the discretization and tolerance parameters. It is also observed that vacuum is more easily formed in 3D than in 2D, in agreement with the remarks in Section 2.1.2.

Similar results were observed for larger values of  $\gamma$ : the vacuum domain increases slightly as  $\gamma$  increases. This is illustrated in Figure 5.4 for the values  $\gamma = 1.4$ , left, and  $\gamma = 2.5$ , right. Note that this behavior with respect to  $\gamma$  is markedly different from the axisymmetric Euler solution for which the case  $\gamma = 1$  (no cavitation) is quite different from the case  $\gamma > 1$ , see [40] and Appendix.

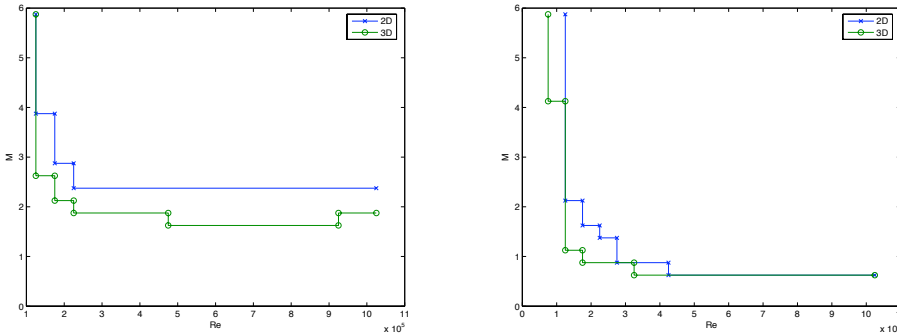


FIG. 5.4. Vacuum formation for two- and three-dimensional barotropic flows (3.13, 3.14) with initial and boundary conditions (3.15, 3.16); left:  $\gamma = 1.4$ , right:  $\gamma = 2.5$ ; vacuum occurs for values of the parameters corresponding to points above the curves.

The code is ill suited for very large values of the Reynolds number (much larger than  $10^6$ ), for which oscillations are found to destroy the accuracy of the method.

**5.3. The full system results.** The results for the full system (3.1-3.3) with boundary condition (3.16) and boundary and initial conditions on the temperature

given by

$$\theta(1, t) = 1, \quad t > 0, \quad (5.2)$$

$$\theta(r, 0) = 1, \quad r > 0, \quad (5.3)$$

are displayed in Figure 5.5. As can be seen in the figure, there again appears to be cavitation for large enough data.

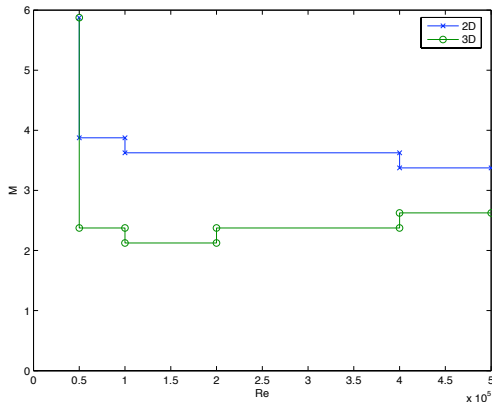


FIG. 5.5. Vacuum formation for two- and three-dimensional Navier-Stokes flows (3.1-3.3) with initial and boundary conditions (3.15, 5.3, 3.16, 5.2),  $\gamma = 1.4$ , and  $\text{Pr} = 1$ ; vacuum occurs for values of the parameters corresponding to points above the curves.

For (much) larger values of the Prandtl number,  $\text{Pr}$ , oscillations in the temperature prevent accurate calculations.

**6. Conclusion.** The numerical results indicate that vacuum formation is possible in solutions of the multi-dimensional compressible Navier-Stokes equations, for discontinuous and sufficiently large data whose density is uniformly bounded away from zero. Those observations do not contradict known results for the 1D Navier-Stokes system, nor the currently known results (for both small and large data) that have been established for multi-D flow.

No attempts were made at following the solutions *past* vacuum formation. The present study also leaves unanswered the issue of whether vacuum formation is instantaneous, as is the case for the corresponding solutions to the Euler equations.

**Acknowledgment.** The last author is indebted to David Hoff for several discussions about the vacuum problem in compressible flow.

#### REFERENCES

- [1] K.E. BRENNAN, S.L. CAMPBELL, L.R. PETZOLD, Numerical solution of initial-value problems in differential-algebraic equations, SIAM Classics in Applied Mathematics, #14, 1996.
- [2] C. CANUTO, M.Y. HUSSAINI, A. QUARTERONI, T.A. ZANG, Spectral methods in Fluid Dynamics, Springer Series Computational Dynamics, Springer, Berlin, 1987.
- [3] C. M. DAFERMOS, *Global smooth solutions to the initial-boundary value problem for the equations of one-dimensional nonlinear thermoviscoelasticity*, SIAM J. Math. Anal. **13** (1982), 397–408.

- [4] C. M. DAFERMOS, L. HSIAO, *Global smooth thermomechanical processes in one-dimensional nonlinear thermoviscoelasticity*, *Nonlinear Analysis, Theory, Methods & Applications*, **6** (1982), 435–454.
- [5] R. DANCHIN, *Global existence in critical spaces for compressible Navier-Stokes equations*, *Inventiones Mathematicae*, **141** (2000) 579–614.
- [6] R. DANCHIN, *Global existence in critical spaces for compressible viscous and heat conductive gases*, *Arch. Rational Mech. Anal.* **160** (2001), 1–39.
- [7] R. DANCHIN, *On the uniqueness in critical spaces for compressible Navier-Stokes equations*, *Nonlinear Differential Equations and Applications* **12** (2005), 111–128.
- [8] R. DUAN, Y. ZHAO, *A note on the non-formation of vacuum states for compressible Navier-Stokes equations*, *J. Math. Anal. Appl.* **311** (2005), 744–754.
- [9] E. FEIREISL, A. NOVOTNÝ, H. PETZELTOVÁ, *On the existence of globally defined weak solutions to the Navier-Stokes equations*, *J. Math. Fluid Mech.* **3** (2001), 358–392.
- [10] E. FEIREISL, *The dynamical system approach to the Navier-Stokes equations of compressible fluids*, *Advances in Math. Fluid Mech.* (Paseky, 1999), 35–66, Springer, Berlin, 2000.
- [11] H. FRID, V. SHELUKHIN, *Vanishing shear viscosity in the equations of compressible fluids for the flows with the cylinder symmetry*, *SIAM J. Math. Anal.* **31** (2000), 1144–1156.
- [12] E. HAIRER, G. WANNER, *Solving ordinary differential Equations II: stiff and differential algebraic problems*, *Springer Series in Computational Mathematics*, #14, Springer, Berlin, 1996.
- [13] D. HOFF, *Spherically symmetric solutions of the Navier-Stokes equations for compressible, isothermal flow with large, discontinuous initial data*, *Indiana Univ. Math. J.* **41** (1992), 1225–1302.
- [14] D. HOFF, *Discontinuous solutions of the Navier-Stokes equations for multidimensional flows of heat-conducting fluids*, *Arch. Rational Mech. Anal.* **139** (1997), 303–354.
- [15] D. HOFF, *Global solutions of the equations of one-dimensional, compressible flow with large data and forces, and with differing end states*, *Z. Angew. Math. Phys.* **49** (1998), 774–785.
- [16] D. HOFF, *Uniqueness of weak solutions of the Navier-Stokes equations of multidimensional, compressible flows*, preprint 2005.
- [17] D. HOFF, H. K. JENSEN, *Symmetric nonbarotropic flows with large data and forces*, *Arch. Rational Mech. Anal.* **173** (2004), 297–343.
- [18] D. HOFF, D. SERRE, *The failure of continuous dependence on initial data for the Navier-Stokes equations of compressible flow*, *SIAM J. Appl. Math.* **51** (1991), 887–898.
- [19] D. HOFF, J. SMOLLER *Non-formation of vacuum states for compressible Navier-Stokes equations*, *Comm. Math. Phys.* **216** (2001), 255–276.
- [20] S. JIANG, P. ZHANG, *Global weak solutions to the Navier-Stokes equations for a 1D viscous polytropic ideal gas*, *Quart. Appl. Math.* **61** (2003), 435 – 449.
- [21] YA. I. KANEL, *A model system of equations for the one-dimensional motion of a gas*, *Differencial'nye Uravnenija* **4** (1968), 721–734.
- [22] S. KAWASHIMA, *Systems of hyperbolic-parabolic composite type, with applications to the equations of magnetohydrodynamics*, PhD Thesis, Kyoto University, 1983.
- [23] S. KAWASHIMA, T. NISHIDA, *Initial-boundary value problems for the equations of motion of compressible viscous and heat-conductive fluids*, *Comm. Math. Phys.* **89** (1983), 445–464.
- [24] B. KAWOHL, *Global existence of large solutions to initial boundary value problems for a viscous, heat-conducting, one-dimensional real gas*, *J. Differential Equations* **58** (1985), 76–103.
- [25] A. V. KAZHIKHOV *Sur la solubilité globale des problèmes monodimensionnels aux valeurs initiales-limitées pour les équations d'un gaz visqueux et calorifère*, *C. R. Acad. Sci. Paris* **284** (1977), Sér. A, 317–320.
- [26] A. V. KAZHIKHOV, V. V. SHELUKHIN, *Unique global solution with respect to time of initial-boundary value problems for one-dimensional equations of a viscous gas*, *J. Appl. Math. Mech.* **41** (1977), 273–282.; translated from *Prikl. Mat. Meh.* **41** (1977), 282–291 (Russian)
- [27] P. L. LIONS, *Mathematical Topics in Fluid Mechanics, Volume 2, Compressible Models*, Oxford, 1998.
- [28] T. P. LIU, Z. XIN, T. YANG, *Vacuum states for compressible flow*, *Discrete Contin. Dynam. Systems* **4** (1998), 1–32.
- [29] T. LUO, Z. XIN, T. YANG, *Interface behavior of compressible Navier-Stokes equations with vacuum*, *SIAM J. Math. Anal.* **31** (2000), 1175–119.
- [30] A. MATSUMURA, T. NISHIDA, *The initial value problem for the equations of motion of viscous and heat-conductive gases*, *Journal of Mathematics of Kyoto University* **20**, (1980) 67–104.
- [31] A. NOVOTNÝ, I. STRAŠKRABA, *Introduction to the Mathematical Theory of Compressible Flow*, Oxford, 2004.
- [32] J. SERRIN, *Mathematical principles of classical fluid mechanics. Handbuch der Physik, Bd. 8/1*,

- Strömungsmechanik I, pp. 125–263, Springer-Verlag, 1959.
- [33] L.F. SHAMPINE, M.W. REICHELT, J.A. KIERZENKA, *Solving index-1 DAEs in MATLAB and Simulink*, SIAM Rev., 3 (1999), 538–552.
- [34] J. SMOLLER, Shock waves and reaction-diffusion equations, Second edition. Grundlehren der Mathematischen Wissenschaften, 258. Springer-Verlag, New York, 1994.
- [35] Z. XIN, *Blowup of smooth solutions to the compressible Navier-Stokes equation with compact density*, Comm. Pure Appl. Math. **51** (1998), 229–240.
- [36] T. YANG, Z. YAO, C. ZHU, *Compressible Navier-Stokes equations with density-dependent viscosity and vacuum*, Comm. Partial Differential Equations **26** (2001), 965–981.
- [37] T. YANG, H. ZHAO, *A vacuum problem for the one-dimensional compressible Navier-Stokes equations with density-dependent viscosity*, J. Differential Equations **184** (2002), 163–184.
- [38] T. YANG, C. ZHU, *Compressible Navier-Stokes equations with degenerate viscosity coefficient and vacuum*, Comm. Math. Phys. **230** (2002), 329–363.
- [39] S.-W. VONG, T. YANG, C. ZHU *Compressible Navier-Stokes equations with degenerate viscosity coefficient and vacuum. II*, J. Differential Equations **192** (2003), 475–501.
- [40] Y. ZHENG, Systems of Conservation Laws: Two-Dimensional Riemann Problems, Birkhauser, 2001.

### Appendix A. The isentropic Euler equations.

The isentropic Euler equations are easily obtained from (3.13, 3.14) by formally taking the limit  $\text{Re} \rightarrow \infty$ , i.e.

$$\rho_t + (\rho u)_\xi = 0, \quad (\text{A.1})$$

$$\rho(u_t + uu_r) + \frac{1}{\gamma M^2}(\rho^\gamma)_r = 0. \quad (\text{A.2})$$

**A.1. The one-dimensional case.** Let us consider (A.1,A.2) together with the Riemann data

$$\rho(r, 0) = 1 \quad \forall r, \quad u(r, 0) = \begin{cases} -1 & \text{if } r < 0, \\ 1 & \text{if } r > 0. \end{cases} \quad (\text{A.3})$$

As is well known, the above Riemann problem can easily be solved. Interestingly, the isothermal case,  $\gamma = 1$ , and the general isentropic case,  $\gamma > 1$ , are quite different.

**A.1.1. The isothermal case  $\gamma = 1$ .** For the “symmetric data” (A.3), the solution is found to consist of two rarefaction waves

$$\begin{bmatrix} \rho \\ u \end{bmatrix} (r, t) = \begin{cases} \begin{bmatrix} 1 \\ -1 \end{bmatrix} & \text{if } \frac{r}{t} < -1 - \frac{1}{M}, \\ \begin{bmatrix} e^{-(M \frac{r}{t} + M + 1)} \\ \frac{r}{t} + \frac{1}{M} \end{bmatrix} & \text{if } -1 - \frac{1}{M} < \frac{r}{t} < -\frac{1}{M}, \\ \begin{bmatrix} e^{-M} \\ 0 \end{bmatrix} & \text{if } -\frac{1}{M} < \frac{r}{t} < \frac{1}{M}, \\ \begin{bmatrix} e^{M \frac{r}{t} - M - 1} \\ \frac{r}{t} - \frac{1}{M} \end{bmatrix} & \text{if } \frac{1}{M} < \frac{r}{t} < 1 + \frac{1}{M}, \\ \begin{bmatrix} 1 \\ 1 \end{bmatrix} & \text{if } 1 + \frac{1}{M} < \frac{r}{t}. \end{cases}$$

Note that regardless of the values of the Mach number,  $M$ , the above solution does not lead to cavitation. Indeed, the smallest value of the density is found to be  $e^{-M}$ .

**A.1.2. The case  $\gamma > 1$ .** Again, the solution is found to consist of two rarefaction waves for the data (A.3). However, in the present case, cavitation can occur. More precisely, if  $M > \frac{2}{\gamma-1}$ , the solution  $[\rho_u](r, t)$  is given by

$$\left\{ \begin{array}{ll} \begin{bmatrix} 1 \\ -1 \end{bmatrix} & \text{if } \frac{r}{t} < -1 - \frac{1}{M}, \\ \begin{bmatrix} \left( \frac{2}{\gamma+1} - M \frac{\gamma-1}{\gamma+1} \left( 1 + \frac{r}{t} \right) \right)^{2/(\gamma-1)} \\ \frac{1}{M(\gamma+1)} \left( 2 + (1-\gamma)M + 2M\frac{r}{t} \right) \end{bmatrix} & \text{if } -1 - \frac{1}{M} < \frac{r}{t} < -1 + \frac{2}{\gamma-1} \frac{1}{M}, \\ \begin{bmatrix} 0 \\ \emptyset \end{bmatrix} & \text{if } -1 + \frac{2}{\gamma-1} \frac{1}{M} < \frac{r}{t} < 1 - \frac{2}{\gamma-1} \frac{1}{M}, \\ \begin{bmatrix} \left( \frac{2}{\gamma+1} + M \frac{\gamma-1}{\gamma+1} \left( -1 + \frac{r}{t} \right) \right)^{2/(\gamma-1)} \\ \frac{1}{M(\gamma+1)} \left( -2 + (-1+\gamma)M + 2M\frac{r}{t} \right) \end{bmatrix} & \text{if } 1 - \frac{2}{\gamma-1} \frac{1}{M} < \frac{r}{t} < 1 + \frac{1}{M}, \\ \begin{bmatrix} 1 \\ 1 \end{bmatrix} & \text{if } 1 + \frac{1}{M} < \frac{r}{t}. \end{array} \right.$$

Note that for this latter solution, no velocity  $u$  is specified in the vacuum. If, on the other hand, the fluid is not sheared as hard, i.e., if  $0 < M < \frac{2}{\gamma-1}$ , then no cavitation takes place and the solution  $[\rho_u](r, t)$  is found to be

$$\left\{ \begin{array}{ll} \begin{bmatrix} 1 \\ -1 \end{bmatrix} & \text{if } \frac{r}{t} < -1 - \frac{1}{M}, \\ \begin{bmatrix} \left( \frac{2}{\gamma+1} - M \frac{\gamma-1}{\gamma+1} \left( 1 + \frac{r}{t} \right) \right)^{2/(\gamma-1)} \\ \frac{1}{M(\gamma+1)} \left( 2 + (1-\gamma)M + 2M\frac{r}{t} \right) \end{bmatrix} & \text{if } -1 - \frac{1}{M} < \frac{r}{t} < -\frac{1}{M} + \frac{\gamma-1}{2}, \\ \begin{bmatrix} \left( 1 - \frac{M}{2}(\gamma-1) \right)^{\frac{2}{\gamma-1}} \\ 0 \end{bmatrix} & \text{if } -\frac{1}{M} + \frac{\gamma-1}{2} < \frac{r}{t} < \frac{1}{M} - \frac{\gamma-1}{2}, \\ \begin{bmatrix} \left( \frac{2}{\gamma+1} + M \frac{\gamma-1}{\gamma+1} \left( -1 + \frac{r}{t} \right) \right)^{2/(\gamma-1)} \\ \frac{1}{M(\gamma+1)} \left( -2 + (-1+\gamma)M + 2M\frac{r}{t} \right) \end{bmatrix} & \text{if } \frac{1}{M} - \frac{\gamma-1}{2} < r/t < 1 + \frac{1}{M}, \\ \begin{bmatrix} 1 \\ 1 \end{bmatrix} & \text{if } 1 + \frac{1}{M} < \frac{r}{t}. \end{array} \right.$$

**A.2. The multidimensional axisymmetric case.** Similarity solutions to the Euler equations can be also be considered for the two and three dimensional axisymmetric problems that are studied in the paper. Even though no closed form solutions can be found, the analysis reveals that solutions without swirls may exhibit cavitation if  $\gamma > 1$  but not if  $\gamma = 1$  [40], §7.4.

**A.3. Other generalizations.** The one-dimensional Riemann problem can also be solved for the nonisentropic Euler equations (full system). Assuming the initial temperature to be equal to 1 everywhere, cavitation is found to occur under exactly the same condition as above ( $M > \frac{2}{\gamma-1}$ ) [34], Theorem 18.6. The construction of self-similar solutions for the nonisentropic Euler equations in the multidimensional axisymmetric case is, to the best of the authors' knowledge, an open problem.